Sensors & Diagnostics

PAPER

View Article Online
View Journal | View Issue

Check for updates

Cite this: *Sens. Diagn.*, 2026, **5**, 76

Lanthanide nanoparticles as ultra-sensitive luminescent probes for quantitative PSA detection *via* lateral flow assays

Juliette Lajoux, [a] Mohamadou Sy,[a] Loïc J. Charbonnière, *[b] Joan Goetz†[a] and Susana Brun †*[a]

Prostate cancer is one of the most common cancers in men, with the PSA (prostate-specific antigen) test serving as a cornerstone for its monitoring and early detection. This study describes the development and evaluation of an innovative quantitative lateral flow assay (LFA) utilizing luminescence from Bright-Dtech™ lanthanide nanoparticles to enhance the sensitivity and accuracy of PSA measurement. The optimized LFA demonstrated high sensitivity and reproducibility, with a detection limit of 15 pg mL^{-1} in buffer (120 pg mL^{-1} in 1 : 8 diluted serum), and a quantifiable range of 0.155 to 27.5 ng mL^{-1} in buffer (1.24 to 221 ng mL^{-1} in 1 : 8 diluted serum). This method was successfully applied for PSA detection in clinical serum samples, and it showed excellent correlation with a quantitative diagnostic reference method. The developed LFA offers a significant advancement in quantitative PSA testing, providing a rapid and cost-effective *in vitro* diagnostic solution. Furthermore, it showcases the potential of Bright-Dtech™ technology in lateral flow test design. With exceptional brightness and long luminescence lifetime, lanthanide nanoparticles effectively address key challenges in LFA sensitivity and quantification, paving the way for broader applications in diagnostic testing.

Received 1st August 2025,
Accepted 22nd October 2025

DOI: 10.1039/d5sd00143a

rsc.li/sensors

Open Access Article. Published on 28 October 2025. Downloaded on 2/13/2026 9:37:28 AM.
This article is licensed under a Creative Commons Attribution 3.0 Unported Licence.

1. Introduction

Rapid diagnostic tests, particularly lateral flow assays (LFAs), have revolutionized early disease detection by providing fast, cost-effective, and easily interpretable results, with a significant impact during the COVID-19 pandemic and beyond.[1] However, their ability to accurately quantify target analytes remains a major challenge. LFAs enable the detection and quantification of analytes in complex samples, such as blood or plasma.[2] These tests operate on the principle of antibody–antigen recognition and rely on a strip composed of various membranes stacked together, allowing the migration of liquid by capillary action.[3] In this context, integrating luminescent lanthanide nanoparticles as detection probes offers a promising approach to improve LFA sensitivity and specificity.[4]

Lanthanide nanoparticles are distinguished by their unique optical properties, including intense luminescence and long luminescence lifetimes.[5,6] These properties allow tracking of nanoparticle luminescence through time-resolved fluorescence (TRF). This method significantly reduces background noise from the biological environment, enabling more specific detection of nanoparticle fluorescence while retaining high-intensity signals and improving the signal-to-noise ratio.[7,8]

Bright-Dtech™ lanthanide nanoparticles overcome the limitations of conventional markers, such as organic dyes, by offering several advantages. These include enhanced brightness, a high molar absorption coefficient, up to 70% luminescence quantum yield, easy coupling with proteins or nucleic acids, availability in multiple colours for multiplexing, biocompatibility and excellent photostability.[9]

Harnessing the enhanced specificity and sensitivity of these nanoparticles, LFAs utilizing lanthanide nanoparticles as detection probes hold considerable potential for a variety of diagnostic applications.

In this study, we demonstrate a proof of concept for the utilization of Bright-Dtech™ nanoparticles in a quantitative LFA designed to detect prostate-specific antigen (PSA), one of the most impactful cancer biomarkers. PSA is a glycoprotein produced by the prostate gland,[10,11] existing in both complexed and free forms in the bloodstream.[12] This study focused on total PSA (tPSA), encompassing both forms. Elevated PSA levels are associated with increased cancer risk, making PSA a valuable marker in assessing patient health.[13] A PSA level exceeding 4 ng mL^{-1} is associated with a 25%

[a] *Poly-Dtech, 204 Avenue de Colmar, 67100 Strasbourg, France.*
E-mail: susana.brun@poly-dtech.com
[b] *Pluridisciplinary Hubert Curien Institute (IPHC, UMR 7178, CNRS/Université de Strasbourg), 25 rue Becquerel, 67087 Strasbourg, France.*
E-mail: l.charbonn@unistra.fr
† These authors contributed equally.

© 2026 The Author(s). Published by the Royal Society of Chemistry

Open Access Article. Published on 28 October 2025. Downloaded on 2/13/2026 9:37:28 AM.
This article is licensed under a Creative Commons Attribution 3.0 Unported Licence.

probability of prostate cancer and is widely recognized as the clinical threshold for diagnostic tests.[10]

PSA testing plays a crucial role in early detection, assessment, and monitoring of prostate cancer progression. However, traditional assays, such as enzyme-linked immunosorbent assays (ELISAs), are time-consuming, require specialized equipment, and depend on trained personnel, limiting their accessibility in resource-limited settings.[14,15] Alternative formats such as lateral flow assays (LFAs) could potentially offer faster and more accessible testing. Although these approaches may still rely on dedicated readers, for example, TRF devices, the growing availability of compact and user-friendly TRF readers makes them increasingly compatible with decentralized use. In this context, the development of quantitative and sensitive LFA methods could contribute to expanding PSA testing beyond centralized laboratories.

By conjugating Bright-Dtech™ nanoparticles with PSA-specific antibodies, we aim to demonstrate the feasibility of this approach for precise and quantitative analyte detection. We evaluate the optimized test's performance in terms of sensitivity, repeatability, reproducibility and accuracy across a relevant concentration range for PSA.

By establishing proof of concept for this sensitive and quantitative LFA utilizing lanthanide nanoparticles luminescence, this study paves the way for advancements in rapid and accurate disease diagnostics. These findings hold significant implications for early prostate cancer detection and improved patient monitoring in clinical settings.

2. Experimental

2.1. Reagents, materials and instruments

Details about the membranes, antibodies, antigen and some instruments are described in the SI. Link-Dtech™ – 614 Europium nanoparticles (EuNPs) conjugation kit was supplied by Poly-Dtech (Strasbourg, France). Conjugation and migration buffers were also provided by Poly-Dtech as part of the Link-Dtech kit. The Western blot module of the SpectraMax ID5 multi-mode microplate reader (Molecular Devices, San Jose, CA, USA) was used to capture fluorescence images of the strips. The images were taken in time-resolved mode with a delay of 50 μs, an integration time of 800 μs, an excitation wavelength of 350 nm, and an emission wavelength of 616 nm. A dark box equipped with UV neon lights (Vilber, Marne-la-Vallée, France) was used to visualize the fluorescence of the bands with the naked eye. Images were also captured with a smartphone under UV light (using a 595 nm filter). The excitation wavelengths emitted by the lamps were 312 ± 20 nm (from 2 UV tubes) and 365 ± 20 nm (from 2 UV tubes).

2.2. Bio-conjugation of lanthanide nanoparticles with detection antibodies

Bright-Dtech™ lanthanide nanoparticles were conjugated with mouse anti-human PSA monoclonal antibodies (mAb1) using the Link-Dtech™ 614 – Eu (red) coupling kit. Briefly, the nanoparticles were sonicated for 2–3 minutes to ensure homogeneous dispersion, and the detection antibodies were then added in a nanoparticle-to-antibody ratio of 1 : 100 (Fig. 1A). After overnight incubation at 4 °C, the conjugated nanoparticles were centrifugated, resuspended in coupling buffer, and subsequently diluted to the working concentration in migration buffer. These conjugates were afterward used in downstream applications. Conjugation efficiency was assessed by quantifying mouse IgG levels with a TR-FRET assay kit before and after the conjugation procedure, to determine the proportion of antibodies bound to the nanoparticles (Fig. S4). The measurement was based on the residual antibody concentration in the supernatant after coupling.

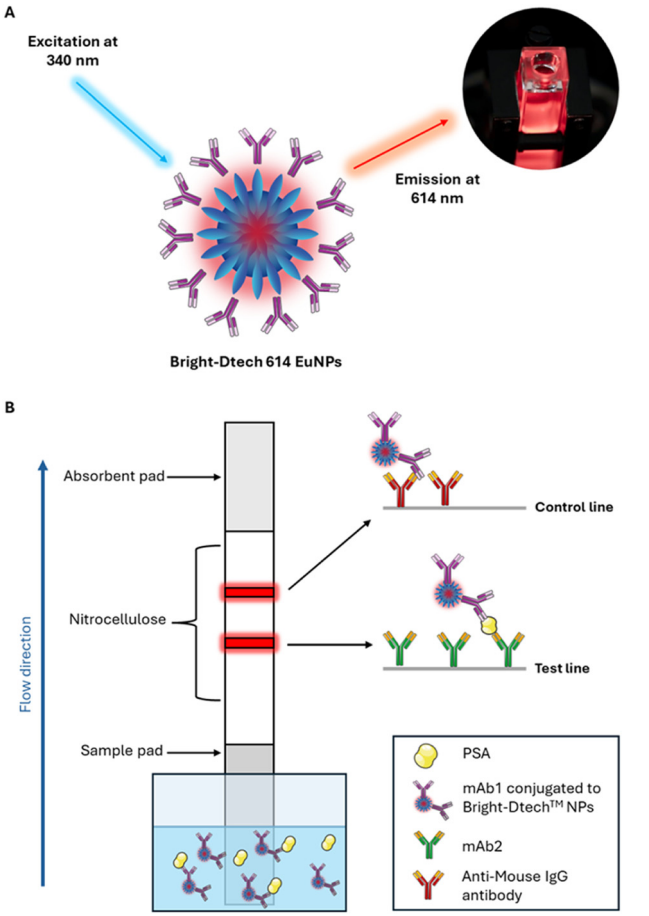

Fig. 1 Lanthanide nanoparticles and their use in LFA. A) Illustration of antibody-conjugated Bright-Dtech™ lanthanide europium nanoparticles (EuNPs). When excited at a wavelength of 340 nm it emits a bright red fluorescent light at 614 nm. B) Schematic illustration of the LFA structure for the detection of PSA using a dipstick assay format. Abbreviations: mAb1, monoclonal antibody 1; mAb2, monoclonal antibody 2.

2.3. Fabrication of LFA strips

LFA strips were assembled using a "dipstick" configuration, comprising a sample pad, nitrocellulose membrane, and absorbent pad, adhered to a backing card (Fig. 1B).

Open Access Article. Published on 28 October 2025. Downloaded on 2/13/2026 9:37:28 AM. This article is licensed under a Creative Commons Attribution 3.0 Unported Licence.

To manufacture the LFA strips, the test line was printed with the mouse anti-human PSA monoclonal antibody (mAb2), while the control line was printed with the anti-mouse IgG polyclonal antibody. Since the interaction time between the different components of the reaction is short, the position of the lines on the membrane is important and must remain constant. In this study, the two lines were separated by a distance of 5 mm and the printing onto the nitrocellulose membrane was performed at a speed of 4.8 mm s^{-1} and a flow rate of 1.5 μL cm^{-1}. Then, the nitrocellulose membrane was dried overnight at room temperature to ensure stability.

The assembly consisted of an absorbent pad (1.8 cm), printed and dried nitrocellulose membrane (2.5 cm) and sample pad (2.3 cm) adhered to a self-adhesive backing (6 cm), overlapping by 1–2 mm for efficient capillary flow. Finally, the assembly was cut into 4 mm-wide strips using the strip cutter.

2.4. Immunochromatographic assay procedure and PSA analytical validation

The "dipstick" method involves depositing the standard PSA or the sample and the antibody-conjugated nanoparticles into a well of a microwell plate and horizontally immersing the test strip throughout the migration process. To quantify the PSA concentration, calibration curve was performed by dispensing 5 μL of conjugated nanoparticles and 75 μL of serial dilutions of standard PSA antigen (0 to 100 ng mL^{-1} in migration buffer) into a 96-well plate. The strips were then immersed in the wells for a 20-minute migration period.

After drying overnight at room temperature, strip images were captured using the Western blot module of the SpectraMax iD5 microplate reader in time-resolved fluorescence mode, which was originally designed for the analysis of Western blot gels. The excitation and emission wavelengths were set to 350 and 616 nm, respectively (Fig. 1A), with an excitation time of 0.05 ms, a delay time of 0.05 ms, and an integration time of 0.8 ms. The fluorescence intensities of nanoparticles at the test and control lines were quantified using the ImageJ software (National Institute of Health, Bethesda, MD). The "gel analysis" tool was applied to convert band intensities into peaks and the area under the curve of each peak was calculated to determine the T/C (test/control) signal ratio and so, determining assay performance.

Data modelling was performed using SoftMax Pro Software (Molecular Devices, Sunnyvale, CA), fitting results to a 5-parameter logistic (5PL) curve. This allowed determination of key analytical parameters, including limit of detection (LOD), lower limit of quantification (LLOQ) and the upper limit of quantification (ULOQ). The LOD, defined as the lowest detectable concentration, is normally calculated as 3 standard deviations (SD) above the blank (negative) control signal. Since no non-specific signal was observed in blank controls, the lowest detected concentration was used instead. The LLOQ and ULOQ were calculated as 10 SD above the lowest concentration value detected and 3 SD below the maximal signal before the plateau, respectively.[16] The dynamic range, corresponding to the interval between LLOQ and ULOQ was established as the quantifiable concentration range for PSA.

The potential cross-reactivity of the assay was evaluated using recombinant human kallikrein-2 (hK2), a structural homologue of PSA and frequent source of analytical interference. hK2 was spiked into human serum either alone or together with PSA at a 10× molar excess. Specificity was assessed through three complementary experiments: (A) cross-reactivity, (B) interference/competition, and (C) spike-and-recovery, as described in the SI.

2.5. Analysis of clinical serum samples

Eleven individual anonymized male sera were obtained from BIOGROUP-CAB (Mandelieu-La-Napoule, France). These sera were also analysed by BIOGROUP-CAB for PSA measurements using their reference method: a direct two-site sandwich chemiluminescent immunoassay (Siemens Healthineers, Courbevoie, France).

For LFA testing, 75 μL of 8-fold diluted serum (*i.e.*, 1 volume of serum +7 volumes of buffer) was added to 5 μL of conjugated nanoparticles into the well. Each sample was analysed in triplicate, and the results are presented as mean values. The recovery rates and clinical applicability of the LFA test were assessed by comparing the results to those obtained with BIOGROUP-CAB's reference method.

2.6. Statistical analysis

Passing–Bablok regression analysis was performed with MedCalc Software (MedCalc, Mariakerke, Belgium). Bland–Altamn plot was performed with GraphPad Prism 6 (GraphPad Software, San Diego, CA, USA). Data was presented as mean value with their standard deviation.

3. Results and discussion

3.1. Calibration curve and analytical performance

Several optimization steps were conducted to establish the ideal conditions for this assay. These parameters included nitrocellulose membrane selection, antibodies concentration, and nanoparticles concentration used throughout the test. The detailed results of these optimization steps are provided in the SI (Fig. S1), and collectively enabled the optimal detection of PSA using a LFA with Bright-Dtech™ nanoparticles. All the subsequent experiments were performed under these optimized conditions. Additionally, the supplementary information includes data on the transmission electron microscopy (TEM) and dynamic light scattering (DLS) characterization of nanoparticle size and shape, as well as fluorescence intensity measurements and DLS results over a two-year period, which confirm the stability of the nanoparticles (Fig. S2 and S3).

The analytical performances of the test were evaluated through a calibration curve, prepared with serial dilutions of PSA in the migration buffer. Fig. 2A shows LFA strips images

© 2026 The Author(s). Published by the Royal Society of Chemistry

Open Access Article. Published on 28 October 2025. Downloaded on 2/13/2026 9:37:28 AM.
This article is licensed under a Creative Commons Attribution 3.0 Unported Licence.

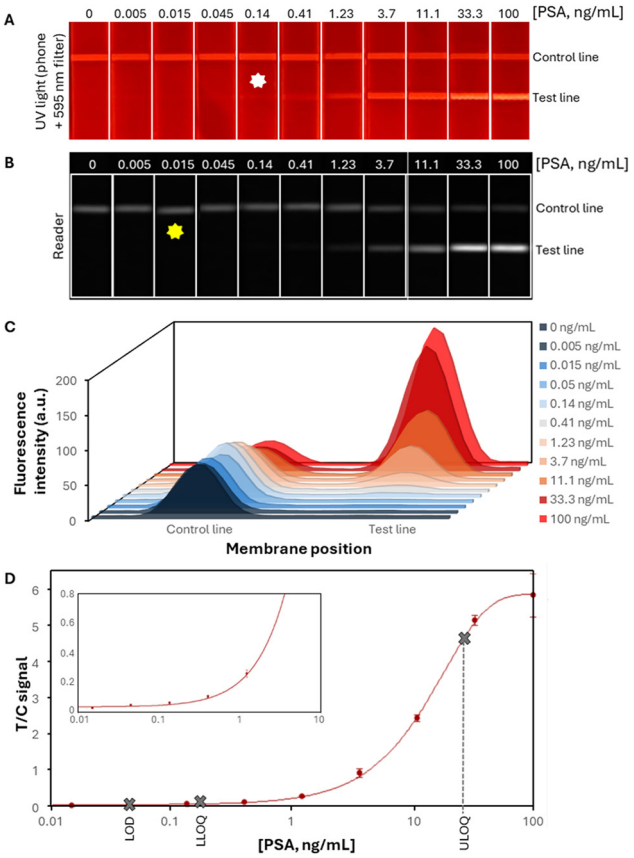

Fig. 2 Analysis of the relationship between the PSA concentration and assay response. (A and B) Typical images captured with a smartphone under UV light (A) and with the reader (B) of strips carried out with two-fold serially diluted PSA standard in migration buffer and a negative control (0 ng mL^{-1} PSA). White and yellow stars indicate the limit of detection as observed with the naked eye and with the reader, respectively. (C) The fluorescence signal intensity of (B) at different positions on the membrane at PSA concentration from 0 to 100 ng mL^{-1} (D) the calibration curve plot of (B) representing the normalized test line by control line (T/C) signal (n = 4).

captured with a smartphone under UV light. An increased red brightness in T line could be clearly observed at very low PSA concentration of 0.14 ng mL^{-1} (white star), based on unanimous visual detection by five individuals using the naked eye, which can be considered as the LOD for visual qualitative detection using our assay.

The same test results were also quantified by a reader under excitation with a 350 nm flash lamp. Fig. 2B–D shows LFA strips image captured with the reader, the fluorescence signal intensity at control and test lines position, and the graph generated with SoftMax Pro software by plotting the T/C signal using a 5PL model, respectively. The resulting calibration curve demonstrated a dose–response relationship, increasing with PSA concentrations, as evidenced by a progressive intensification of the test line. Signal saturation was observed at 100 ng mL^{-1} of PSA.

Key analytical parameters were derived, including LOD, LLOQ and ULOQ. The resulting calibration curve demonstrated a R^2 of 1.00, confirming the model's suitability

Table 1 Repeatability (intra-assay CV%) and reproducibility (inter-assay CV%) results

Dose (ng mL^{-1})	Intra-assay CV%	Inter-assay CV%
35	6%	11%
10	8%	11%
2	8%	15%

Abbreviation: CV%, coefficient of variation percentage.

for PSA quantification. Notably, no blank (non-specific binding) signal was detected, highlighting the test's specificity but necessitating alternative LOD determination methods. Therefore, to calculate the LOD, we applied the approach commonly used in qualitative tests, which identifies the lowest PSA concentration capable of producing a detectable signal distinguishable from the blank.[17] The lowest detectable PSA concentration was 15 pg mL^{-1} (yellow star in Fig. 2B) reflecting the strong performance of the developed test. The LLOQ and ULOQ were 0.155 ng mL^{-1} and 27.5 ng mL^{-1}, respectively, defining a dynamic range suitable for precise PSA quantification (Table S1). These sensitivities surpass the clinical threshold of 4 ng mL^{-1}, enabling accurate PSA detection even in diluted samples. Such precision supports early cancer detection and patient monitoring.

The test also demonstrated robust repeatability and reproducibility, with intra-assay and inter-assay coefficients of variation (CV) below 10% and 15%, respectively, at three different concentrations of PSA tested in 4 replicates (Table 1).

Given the structural homology between PSA and human kallikrein-2 (hK2), we evaluated potential cross-reactivity and interference. As shown in supplementary information (Fig. S5), hK2 spiked into human serum at 10× molar excess generated no measurable signal (≤0.5% cross-reactivity) and did not alter PSA quantification. Spike-and-recovery experiments confirmed that PSA recovery remained within the predefined 80–120% acceptance range even in the presence of high hK2.

Taken together, these results confirm that the assay provides consistent and reproducible PSA quantification with robust specificity.

3.2. Impact of the matrix

To assess the applicability of the assay to complex samples, sera from 11 patients were analysed with the LFA strips. PSA levels in these samples were pre-determined using a reference chemiluminescent two-site sandwich immunoassay (Siemens). For application in our assay, serum samples were diluted 8-fold to provide optimal nanoparticle migration along the strip and signal quantification. Importantly, no matrix effect was observed and PSA levels measured with the strips were consistent with reference method results, achieving recovery rates between 96 and 114% (Table 2).

To assess and provide insights into the accuracy and reliability of the LFA test for clinical applications, statistical analyses were performed. The Passing–Bablok regression

Open Access Article. Published on 28 October 2025. Downloaded on 2/13/2026 9:37:28 AM. This article is licensed under a Creative Commons Attribution 3.0 Unported Licence.

Table 2 Comparison of PSA concentrations, including recovery rates across different patient samples. Expected recovery values in immunoassays typically range between 80% and 120%

Sample #	SIEMENS reference method [PSA, ng mL^{-1}]	This work [PSA, ng mL^{-1}]	% recovery
1	<4	<LOD	—
2	5.4	6.1	112%
3	38.8	37.3	96%
4	4.9	5.5	113%
5	22.9	24.9	109%
6	28.64	31.4	110%
7	<4	<LOD	—
8	95.5	98.2	103%
9	23	25.5	111%
10	5.0	5.7	114%
11	5.4	6.2	114%

analysis (Fig. 3A) showed an intercept of 0.17 (95% CI: −0.3387 to 0.05873), a slope of 1.0849 (95% CI: 1.0204 to 1.1272), and a R^2 of 0.998 with a $p < 0.0001$, indicating a close agreement between the reference and new methods for PSA measurement. The slope near 1 suggests that the new method's measurements are almost equivalent to the reference method and the positive intercept indicates a very small bias in the new method. The Bland–Altman analysis (Fig. 3B) further confirmed this, revealing a mean bias of 1.02 ng mL^{-1} and a mean relative bias of 4.9%, indicating a small but consistent deviation between the two methods below 10%. The findings suggest that while the new method is highly correlated with the reference method, the observed bias is acceptable within the context of clinical applications and demonstrates the assay's potential for detecting PSA directly in serum without compromising accuracy or consistency.

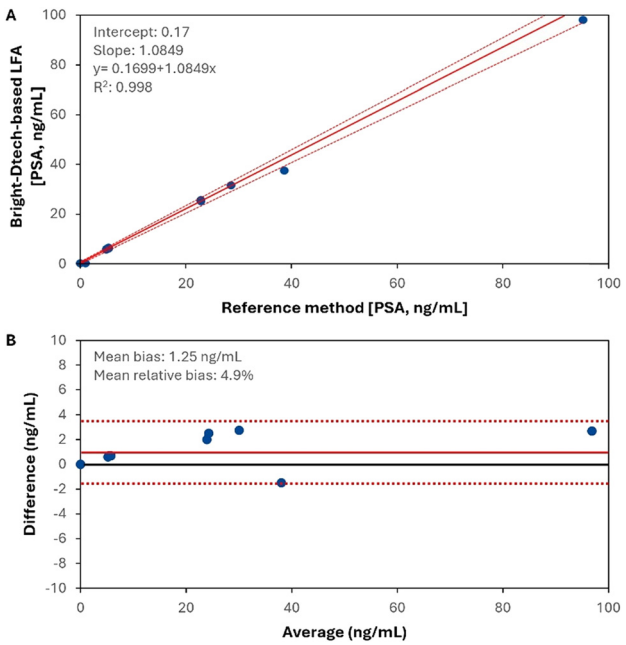

Fig. 3 Comparison of the developed Bright-Dtech-based LFA and the reference method for PSA detection. (A) Correlation curve between the pre-determined results using a reference method (from BIOGROUP) and the proposed method here using the Passing–Bablok regression analysis. The red solid line represents the regression line, with the dashed lines indicating the 95% confidence intervals for the intercept and slope. (B) Bland–Altman plot of the difference *versus* the average of two methods, illustrating their agreement and bias. The *x*-axis represents the average of the two methods, and the *y*-axis represents the difference between the methods. The dashed lines represent the 95% limits of agreement, with the red solid line indicating the mean bias.

3.3. Comparison of PSA detection methods

Table 3 compares the Bright-Dtech-based LFA developed in this study with other PSA detection methods, focusing on assay time, sensitivity, and applicability to point-of-care testing (POCT). Conventional methods, such as chemiluminescent two-site sandwich immunoassay and ELISA, offer exceptional sensitivity with LODs of 0.01 ng mL^{-1} and 0.008 ng mL^{-1}, respectively. However, these methods are unsuitable for POCT due to their lengthy assay times (while some ELISA protocols may take as little as 90 minutes, most tests require more than 3 hours) and the requirement for certain laboratory conditions and skilled staff.

Classical point-of-care methods, such as gold nanoparticle-based LFAs, provide rapid results (≈20 minutes). However, their semi-quantitative nature limits the precision of PSA measurements, making them less suitable for clinical scenarios requiring accurate quantification.

Luminescent nanoparticle-based methods have emerged as promising alternatives, combining high sensitivity with the practicality required for POCT. For example, LFA using quantum dot nanobeads[18] or europium nanoparticles[19] enable quantitative and sensitive PSA detection with LODs comparable to those achieved in this study. However, these assays are not yet commercially available, restricting their accessibility and widespread adoption.

In contrast, the LFA developed here achieves a LOD of 0.015 ng mL^{-1} offering sensitivity comparable to ELISA but with a significantly reduced assay time of just 20 minutes. This makes it highly practical for rapid diagnostic applications. Furthermore, Bright-Dtech™ nanoparticles are already commercially available, facilitating adoption by researchers and laboratories.

Lanthanide nanoparticles, such as those used in this study, offer additional advantages over other nanoparticles, such as quantum dots or gold NPs.[20] These advantages include enhanced fluorescence intensity, superior stability, and improved signal detection, particularly in LFA formats. These properties make our LFA particularly well-suited for POCT environments, where sensitivity, robustness, and reliability are critical.

4. Conclusion

The objective of this project was to develop and evaluate the performances of a lateral flow test based on the luminescence of lanthanide nanoparticles for the quantification of PSA. This study successfully demonstrated a proof of concept for the

© 2026 The Author(s). Published by the Royal Society of Chemistry

Open Access Article. Published on 28 October 2025. Downloaded on 2/13/2026 9:37:28 AM. This article is licensed under a Creative Commons Attribution 3.0 Unported Licence.

Table 3 Comparison of developed Bright-Dtech-based LFA with other methods for PSA detection

Detection method	LOD (ng mL^{-1})	Assay time (min)	Applicability on point-of-care	Ref.
Chemiluminescent two-sites sandwich immunoassay	0.01	18	NO	Siemens, datasheet[a]
ELISA	0.008	90	NO	Sigma-Aldrich, datasheet[b]
Gold NPs-based LFA	>4	20	YES	Biogatelab, datasheet[c]
Quantum dots nanobeads-based LFA	0.14–0.33	15	YES	10,18
EuNPs-based LFA	0.07–0.08	40	YES	19
Bright-Dtech-based LFA	0.015	20	YES	This work

Abbreviations: ELISA, enzyme-linked immunosorbent assay; NPs, nanoparticles; LFA, lateral flow assay; Eu, Europium; LOD, Limit of detection. [a] Siemens, "Atellica IM Prostate-Specific Antigen (PSA) Datasheet." Available at: https://doclib.siemens-healthineers.com/rest/v1/view?documentid=939791 (accessed Dec. 17/2024). [b] Sigma-Aldrich, "Human PSA-total ELISA Kit Datasheet." Available at: https://www.sigmaaldrich.com/deepweb/assets/sigmaaldrich/product/documents/380/803/rab0331ugrev0824-mk.pdf (accessed Dec. 17/2024). [c] Biogatelabs, "One Step PSA Rapid Test Datasheet." Available at https://biogatelab.com/uploads/3/4/4/1/34413460/psa_triline_cassette.pdf (accessed Dec. 17/2024).

sensitive and accurate quantification of PSA using commercially available Bright-Dtech™ 614-Eu nanoparticles. The developed test holds significant promise for the early detection and monitoring of prostate cancer and other prostate-related diseases.

Validation studies, including the establishment of a standard curve, intra- and inter-assay evaluations, and analysis of clinical samples, confirmed the test's repeatability, reproducibility, and accuracy from very low PSA concentrations in 1 : 8 serum. While this study focuses primarily on the technical development and analytical performance of the assay, initial validation with clinical serum samples demonstrates promising applicability. Expanding the clinical study cohort is part of our future plans and will help further assess diagnostic performance across a wider range of PSA levels. The assay reliably quantifies PSA above 0.155 ng mL^{-1} (minimum quantifiable in 1 : 8 diluted serum of 1.24 ng mL^{-1}) with an impressive LOD of 0.015 ng mL^{-1} (minimum detectable in 1 : 8 diluted serum of 0.12 ng mL^{-1}).

The developed test combines several advantages: it is quantitative, nearly as sensitive as conventional PSA detection methods (ELISA, chemiluminescent immunoassay), and offers a significant reduction in assay time (20 minutes *versus* several hours for traditional ELISA protocols, which often require 3–4 hours due to extended incubation and washing steps).

The developed test combines several advantages: it is quantitative, nearly as sensitive as conventional PSA detection methods (ELISA, chemiluminescent immunoassay), and offers a significant reduction in assay time (20 minutes *versus* several hours for traditional ELISA protocols, which often require 3–4 hours due to extended incubation and washing steps).

The use of Bright-Dtech™ nanoparticles, which are readily available on the market, enables the rapid and efficient development of ultra-sensitive quantitative LFA. This accessibility eliminates the need for extensive expertise in inorganic chemistry or nanotechnology to synthesize, characterize, and conjugate these signal reporters with bioreceptors, making the technology more accessible to researchers and laboratories.

Furthermore, recent advances in compact, portable TRF readers, including benchtop, battery-powered, and even smartphone-integrated devices, support the feasibility of deploying TRF-based LFAs in decentralized or point-of-care settings.

In conclusion, the integration of Bright-Dtech™ nanoparticle technology with lateral flow test platforms addresses key challenges in *in vitro* diagnostics. This approach provides a simple, rapid, and sensitive solution for analyte quantification, paving the way for improved patient care. The development of these tests has the potential to enhance disease monitoring, to enable earlier diagnosis, and thus to reduce the risk of mortality, disability, and the need for intensive treatments.

Author contributions

J. L.: project administration, investigation, methodology, formal analysis, validation, writing – original draft. M. S.: project administration, conceptualization, supervision, methodology, formal analysis, validation and review. L. C.: project administration, conceptualization, validation and review. J. G.: project administration, conceptualization, funding and review. S. B.: project administration, conceptualization, supervision, validation and writing – review & editing. All authors have contributed and given approval to the final version of the manuscript.

Conflicts of interest

The authors declare that J. L., M. S., and S. B. are employees of Poly-Dtech, and that J. G. is both an employee and a co-founder of the company. L. C. is also a co-founder of Poly-Dtech. The company holds a patent on Bright-Dtech™ nanoparticles and commercializes the Link-Dtech™ 614 – Eu conjugation kit.

Data availability

The supplementary information (SI) includes additional experimental details, materials and methods, and supporting data related to the development, characterization, and

Open Access Article. Published on 28 October 2025. Downloaded on 2/13/2026 9:37:28 AM.
This article is licensed under a Creative Commons Attribution 3.0 Unported Licence.

analytical performance of the EuNPs-based LFA for PSA detection. Supplementary information is available. See DOI: https://doi.org/10.1039/d5sd00143a.

References

1 J. Budd, B. S. Miller, N. E. Weckman, D. Cherkaoui, D. Huang, A. T. Decruz, N. Fongwen, G.-R. Han, M. Broto, C. S. Estcourt, J. Gibbs, D. Pillay, P. Sonnenberg, R. Meurant, M. R. Thomas, N. Keegan, M. M. Stevens, E. Nastouli, E. J. Topol, A. M. Johnson, M. Shahmanesh, A. Ozcan, J. J. Collins, M. Fernandez Suarez, B. Rodriguez, R. W. Peeling and R. A. McKendry, *Nat. Rev. Bioeng.*, 2023, **1**, 13–31.
2 K. M. Koczula and A. Gallotta, *Essays Biochem.*, 2016, **60**, 111–120.
3 A. N. Danthanarayana, E. Finley, B. Vu, K. Kourentzi, R. C. Willson and J. Brgoch, *Anal. Methods*, 2020, **12**, 272–280.
4 F. Zhang, M. Zou, Y. Chen, J. Li, Y. Wang, X. Qi and Q. Xue, *Biosens. Bioelectron.*, 2014, **51**, 29–35.
5 L. Zhang, Y. Mazouzi, M. Salmain, B. Liedberg and S. Boujday, *Biosens. Bioelectron.*, 2020, **165**, 112370.
6 U. Cho and J. K. Chen, *Cell Chem. Biol.*, 2020, **27**, 921–936.
7 J. Goetz, A. Nonat, A. Diallo, M. Sy, I. Sera, A. Lecointre, C. Lefevre, C. F. Chan, K. Wong and L. J. Charbonnière, *ChemPlusChem*, 2016, **81**, 526–534.
8 C. Charpentier, V. Cifliku, J. Goetz, A. Nonat, C. Cheignon, M. Cardoso Dos Santos, L. Francés-Soriano, K. Wong, L. J. Charbonnière and N. Hildebrandt, *Chem. – Eur. J.*, 2020, **26**, 14602–14611.
9 K.-L. Wong, J. Goetz, L. Charbonniere, N. Hildebrandt, A. Nonat, C. Charpentier, M. Cardoso Dos Santos and V. Cifliku, European Union, EP3591024B1, 2021.
10 S. Bock, H.-M. Kim, J. Kim, J. An, Y.-S. Choi, X.-H. Pham, A. Jo, K. Ham, H. Song, J.-W. Kim, E. Hahm, W.-Y. Rho, S. H. Lee, S. Park, S. Lee, D. H. Jeong, H.-Y. Lee and B.-H. Jun, *Nanomaterials*, 2021, **12**, 33.
11 H. Lilja, A. T. K. Cockett and P.-A. Abrahamsson, *Cancer*, 1992, **70**, 230–234.
12 H. Lilja, A. Christensson, U. Dahlén, M. T. Matikainen, O. Nilsson, K. Pettersson and T. Lövgren, *Clin. Chem.*, 1991, **37**, 1618–1625.
13 A. Heidenreich, G. Aus, M. Bolla, S. Joniau, V. B. Matveev, H. P. Schmid and F. Zattoni, *Eur. Urol.*, 2008, **53**, 68–80.
14 H. Hsieh, J. Dantzler and B. Weigl, *Diagnostics*, 2017, **7**, 29.
15 B. O'Farrell, in *Lateral Flow Immunoassay*, ed. R. Wong and H. Tse, Humana Press, Totowa, NJ, 2009, pp. 1–33.
16 R. Minic and I. Zivkovic, in *Norovirus*, ed. G. Mózsik, IntechOpen, 2021.
17 G. Ross, M. Bremer, J. Wichers, A. Van Amerongen and M. Nielen, *Biosensors*, 2018, **8**, 130.
18 X. Li, W. Li, Q. Yang, X. Gong, W. Guo, C. Dong, J. Liu, L. Xuan and J. Chang, *ACS Appl. Mater. Interfaces*, 2014, **6**, 6406–6414.
19 E. Juntunen, T. Myyryläinen, T. Salminen, T. Soukka and K. Pettersson, *Anal. Biochem.*, 2012, **428**, 31–38.
20 S. Lee, M. Lin, A. Lee and Y. Park, *Nanomaterials*, 2017, **7**, 411.

© 2026 The Author(s). Published by the Royal Society of Chemistry